Reliability Engineering and System Safety 213 (2021) 107682

Contents lists available at ScienceDirect

Reliability Engineering and System Safety

journal homepage: www.elsevier.com/locate/ress

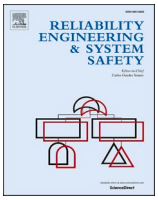

Techno-economic hardening strategies to enhance distribution system resilience against earthquake

Balaji Venkateswaran V *, Devender Kumar Saini, Madhu Sharma

Electrical and Electronics Engineering Department, University of Petroleum and Energy Studies, Dehradun, Uttarakhand 248007 India

ARTICLE INFO

Keywords:
Distribution System Hardening
Energy Storage Units (ESUs)
Power System Planning
Earthquakes
Resilience

ABSTRACT

The electrical distribution grid is unremittingly vulnerable to natural disasters. Many researchers propose strategies mainly based on grid-side solutions to improve critical load's survivability during the targeted emergency period. However, the main agenda of resilience enhancement is to improve the overall system resilience. Therefore, this paper proposes a proactive framework that combines the grid-side and demand-side solutions to enhance the overall system resilience. Here, the grid-side approach presents optimal hardening of the distribution grid by using resilient energy storage units (ESUs), underground cables (UCs), and the demand-side by using home battery inverters (HBIs) & its communication infrastructure. For resilient hardening against earthquakes, it is essential to identify it's all possible occurrences. Therefore, a Monte-Carlo-based probabilistic earthquake hazard model is developed through which the vulnerability is characterized using the peak ground acceleration (PGA) model and fragility curves. For optimized hardening investments, the vulnerable zones of the system are identified via clustering algorithms. With the formulated mixed-integer nonlinear problem, the optimal ESUs and UCs are identified for each cluster. The proposed methodology is tested on a real-world 156-bus distribution system of Dehradun district, India, under seismic zone IV.

1. Introduction

In recent years, the integration of renewable energy resources into the distribution grid is increasing; and the uncertainty of power generation from renewable plants led to the integration of energy storage units (ESUs) to increase the grid flexibility [1–4]. Besides, direct integration of ESUs into the distribution grid poses various advantages like reliability enhancement, peak management, etc. For example, in India, TATA Power Delhi Distribution Limited (TPDDL) has established an ESU with a size of 10MW at Rohini Substation to enhance the grid flexibility [5]. Since the installation of ESUs will fetch a considerable capital investment for utility companies, an optimal number of ESUs are identified, which can enhance the grid flexibility and the overall cost [6–9]. On the other side, the frequency of natural disasters has increased significantly compared to the past [10,11]. In the United States, massive blackouts are caused by natural disasters like hurricanes. A recent study shows that hurricane Harvey hugely affected the transmission system's tower-line link, which caused a complete blackout in the region [12]. Likewise, in 2015 the livelihood of people from Chennai, India has been affected by the floods, mainly due to improper planning [13]. Therefore, the situation demands the power system planners to develop a resilient grid that can serve at least part of its load during emergency condition.

A resilient grid's main idea is to serve the demand without much change in the system performance, even during an event. The concept of enhancing power system resilience is in its initial phase, and there is a need to create awareness and raise fund for the utility. Therefore, the notion of a resilient power grid is restricted to serve at least critical loads such as hospitals, water pump houses, community centers (where the disaster affected people are accommodated) and priority loads. The ideal expectation and the practical system performance while pre-event, during the event, and post-event, respectively, is shown in Fig. 1 [14].

Various strategies have been developed in the literature to improve the system resilience which is dependent on the type of disaster such as floods, hurricanes, landslides, earthquakes, etc. [15–17]. The strategies developed are mainly based on grid-side solutions by hardening the grid, i.e. by replacing the distribution system poles that are vulnerable to disaster, mobilizing the repair crew, etc., and operational enhancement by installing of optimal sectionalizers for feasible microgrids with the available resources [18]. Considering the overall expenditure required to harden the system, many researchers have proposed various optimal

* Corresponding author.
E-mail address: balajivenkateswaran.v@gmail.com (B. Venkateswaran V).

https://doi.org/10.1016/j.ress.2021.107682
Received 22 December 2020; Received in revised form 28 February 2021; Accepted 3 April 2021
Available online 11 April 2021

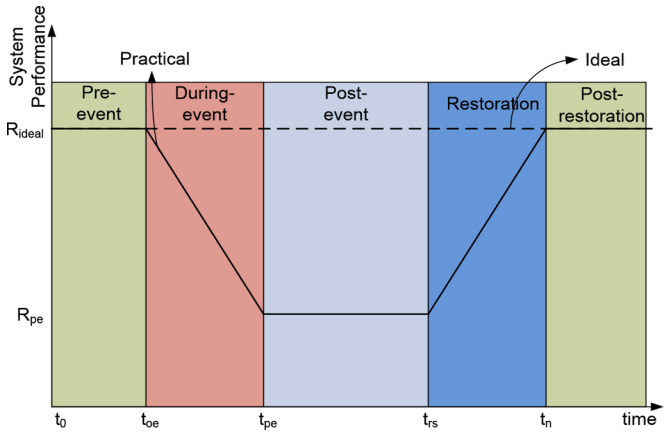

Fig. 1. Ideal and Practical Resilience Curve.

solutions to minimize the overall investment to enhance system resilience [19]. For example, one way is to improve transmission system resilience by expanding its capacity. However, considering the investment, an optimization problem is formulated, which minimizes the cost of capacity expansion and cost for installing switches [20].

Similarly, a mixed-integer linear programming (MILP) model is proposed to enhance distribution system flexibility under common faults. Here, the optimization problem is formulated to minimize the cost of sectionalizers and energy not supplied, respectively constrained with budget limitations [21]. For a better operation of the prior installed sectionalizer switches, a methodology is proposed based on graph theory which identifies the optimal path to satisfy the demand using greedy algorithm [22]. Alternatively, a framework is proposed to effectively utilize temporary distributed generators meeting the demand during the emergency and normal conditions [23]. In [24], the authors have optimized the power generation from solar PV and the ESU by developing various scenarios of extreme events affecting the transmission system to improve its resilience without considering the vulnerability of solar PV and ESU against the disaster. To enhance system resilience, many authors proposed various methodologies for effective utilization of prior installed REPs and ESUs [25–33]. However, in these methodologies, there are possibilities of REPs and ESUs failing to supply the expected energy demand (EED) during the event because of the following: (i) failure of connected substations, (ii) failure of distribution lines connecting the critical demand, and (iii) failure of REPs and/or ESUs. Therefore, it is essential to consider the vulnerability of electrical infrastructure against the disaster.

In general, the vulnerability of infrastructure depends on the type of disaster; therefore, its assessment is disaster-dependent. For example, to assess an electric pole's withstanding capability against the high-speed wind, it is essential to derive its failure probability for a given wind speed. This failure probability is generally obtained by using fragility curves which are infrastructure and disaster specific. A damage modelling framework is proposed to enhance the system resilience against high wind speed by utilizing the fragility curves to estimate the failure probability of electric poles [34,35]. Here, to improve the estimation of damage probability obtained from fragility curves, the same is calibrated based on the past data's empirical relationship. With the concept of fragility curves for distribution lines against earthquake, a framework is proposed to identify the optimal capacity of ESU, which can satisfy the energy demand of limited critical loads [36]. Considering the capital investment, the installation of ESUs to serve the demand during a high impact low probability (HILP) event is highly debatable. After a natural disaster, it is essential to operate the ESUs to satisfy the required demand optimally. An optional operational strategy based on fuzzy logic is proposed to enhance system resilience [28]. A resilience cut is proposed to ensure the desired state of charge (SOC) level of the placed ESUs for

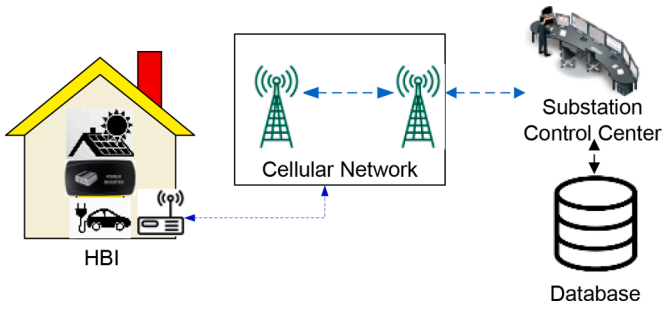

Fig. 2. Communication Infrastructure for HBIs.

serving the emergency period's demand during the pre-disaster period [30]. As mentioned earlier, system restoration after the disaster is very crucial in determining system resilience.

Regarding this, a mathematical model for infrastructure recovery (both physical and service) is proposed based on repair crew management and fragility curves against earthquakes [37]. Here, the model essentially describes a component's vulnerability against a disaster and its state of operation during the disaster. In [38], the importance and the impact of ESU planning strategies on resilience are discussed. Here, a generalized methodology based on the area of resilience trapezoid is proposed (by the authors of this paper) for optimal planning of ESUs to enhance system resilience.

The literature review shows that many authors mainly focused on grid-side strategies leaving behind the demand-side resilience. Moreover, the methodologies that consider the available REPs and ESUs to enhance system resilience fail to consider these infrastructure's vulnerability against disaster. The methods that consider the vulnerability of electrical infrastructure (mainly distribution lines) fail to consider the vulnerability of REPs, ESUs and the substations to which it connected. Therefore, it is essential to redesign the ESU planning strategies adaptable to both normal and extreme conditions. Hence, this paper proposes a framework that includes both grid-side and demand-side resilience strategies to improve distribution system's overall resilience. In this study, to address grid-side hardening strategy, ESUs and UCs are considered and to address demand-side strategy, home battery inverters (HBIs) are considered. The HBI constitutes of BIS, solar rooftop plants, and electric vehicles. Here, the cost of the communication infrastructure of HBI (shown in figure 2) is included in the optimization problem to make it three-dimensional thereby to enhance the overall system resilience. In other words, the three-dimensional hardening provides the effectual capacity addition and the optimal operation of ESUs, considering the available power from REPs and HBIs will enhance the overall resilience of the distribution grid. Various heuristic algorithms are applied in the literature to solve similar optimization problem (i.e., placement of renewable-based distributed generators). Among those, the PSO algorithm provides a better solution with faster convergence and a higher probability to find the global minima.

In contrast, algorithms like ant colony optimization (ACO), harmony search (HS), simulated annealing (SA) suffers from premature convergence, dependence on initial configuration, uncertain convergence time, change of variable distribution at each iteration, etc., [39]. Therefore, in this article, a hybrid algorithm based on adaptive particle swarm optimization (APSO) and binary particle swarm optimization (BPSO) is applied [40]. Besides, the choice of ESUs is made by considering their impact on the environment. The natural disaster considered in this study is the earthquake. Therefore, a practical 156-bus distribution system of Dehradun district, Uttarakhand, India, which comes under seismic zone IV, is chosen to validate the effectiveness of the proposed methodology [41].

The main contributions of this paper are:

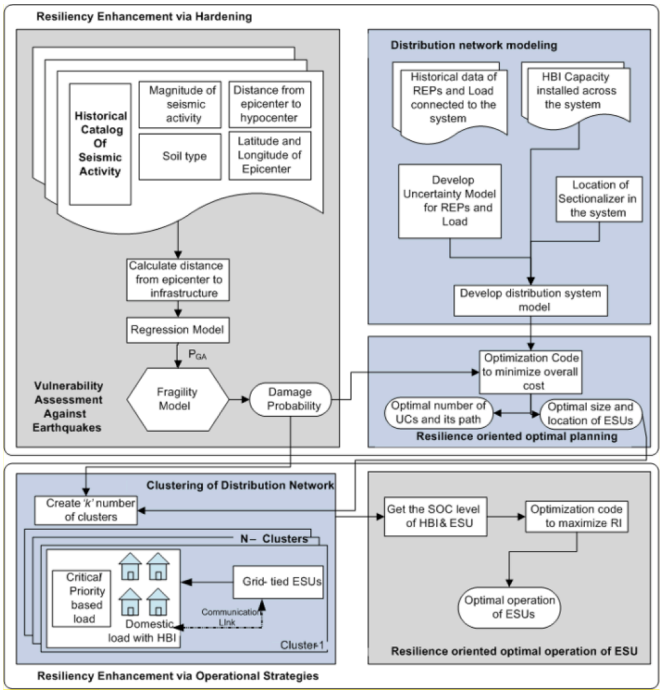

Fig. 3. Overall representation of the proposed framework.

1 A proactive framework to enhance system resilience by considering both grid-side and demand-side solutions.
2 Monte-Carlo based Probabilistic Earthquake hazard model for generating all possible occurrences of seismic activity within the chosen location and thereby estimating all possible failure probabilities of substations and distribution lines.
3 Clustering the network into vulnerable zones and identifying the required three-dimensional hardening to enhance the overall system resilience.

To implement the proposed methodology, it is essential to collect the required data, such as the density of various components of HBIs across the network and the historical seismic activity data for the chosen region. Therefore, a survey is conducted to gather all the data as mentioned earlier. The numerical experiments are performed by linking DigSILENT PowerFactory and Python, where DigSILENT PowerFactory is used to develop the distribution network, and Python is used to implement the proposed methodology. Section 2 elaborates on the proposed framework. Section 3 explains the characterization of earthquakes and the Monte-Carlo based probabilistic earthquake hazard model. Section 4 describes the optimization problem for three-dimensional hardening and optimal operation of ESUs during ERT. The proposed methodology to solve the formulated problem enhance the resiliency of the distribution network is discussed in section 5. The results obtained by implementing the proposed methodology on a real-world system by considering two schemes are elaborated in section 6. Section 7 interprets the critical findings of this paper, and section 8 concludes the article.

2. Proposed framework

This section elaborates the proposed proactive framework, which combines both grid-side and demand-side resilience shown in figure 3. As mentioned earlier, ESUs and UCs are considered under grid-side, and HBIs distributed across the distribution system are considered under demand-side resilience enhancement strategy.

2.1. Resilience enhancement via hardening

Concerning resilience enhancement, it is essential to perform vulnerability studies of hardening infrastructure. Since hardening the grid particularly to increase the system resilience will increase the investment, this paper proposes a three-stride hardening methodology to improve both system resilience and flexibility as follows:

Vulnerability Assessment against Earthquakes: The earthquake data considered in this study contains the moment magnitude of the earthquake, its location (latitude and longitude), and the distance from the epicenter to the hypocenter. The ground acceleration due to an earthquake gets attenuated as it travels along with various soil types. Therefore, it is essential to consider the soil type in the seismic model. In this paper, the peak ground acceleration (PGA) model derives the effect of seismic activity on electrical infrastructure (both substation and distribution lines) through an analytical relationship. The algorithm to estimate the potential risk due to seismic hazard is as follows:

i From the seismic catalogue of the chosen region, categorize the severe earthquake magnitude (M_w).
ii Determine the soil type, distance from the epicenter to the hypocenter, and infrastructure location, respectively.
iii Based on the chosen region's historical data, develop a regression model that reflects the relationship of attenuation [42].
iv The standard fragility curves developed by the Federal Emergency Management Agency (FEMA) for electrical infrastructures, and the developed regression model, estimate the potential damage probability [43].

A detailed explanation of earthquake characterization and vulnerability assessment is discussed in section 3.

- *Distribution network modelling:* The modelling of the distribution network aligned with the chosen problem is essential. In other words, it is necessary to model the system with available energy resources (both grid-side and demand-side). In this article, the optimal planning of ESUs and UCs is considered under grid-side resources, which can enhance the system performance during both normal and emergency conditions. The HBIs having BIS, solar rooftop PV and electric vehicles are considered under demand-side energy resources (depending on its availability). For better system hardening to improve overall system resilience, the cost of communication infrastructure between HBIs and the control centre is included in the formulated objective function for optimal hardening. Here, the HBI is modelled as a load during the normal condition and as a demand-side energy resource during emergency conditions. Therefore, the distribution system is modelled with domestic loads (with HBIs obtained from the survey) and the uncertainties associated with REPs and load. The beta and normal distribution function is given by (1) and (2) are assumed to represent the uncertainties associated with REPs and load, respectively [44,45].

$$PDF_{PV}(x_i) = \begin{cases} \frac{1}{\mathrm{B}(\alpha,\beta)} \times x_i^{\alpha-1} \times (1-x_i)^{\beta-1} \; if \; x_i \in [0,1] \\ 0 \; otherwise \end{cases} \quad (1)$$

$$PDF_D(P_i) = \frac{1}{\sqrt{(2\pi)}\sigma[P_i]} \times e^{-(P_i-\mathrm{E}(P_i))\sqrt{2}\sigma[P_i])^2} \quad (2)$$

where the subscripts *PV* and *D* represents the solar PV plants and load connected to the system. x_i represents the power generation from the solar PV power plant, and P_i represents the power demand.

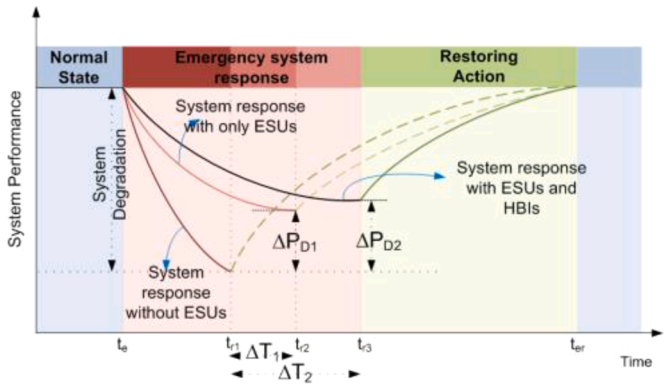

Fig. 4. System Performance against natural disaster: without ESUs, with only ESUs, with ESUs and HBIs.

- *Optimal planning for Hardening:* This paper proposes a three-dimensional hardening procedure in which the formulated objective function consists of cost corresponding to ESUs, UCs and communication infrastructure of HBIs. Minimizing this objective function provides the optimal hardening of the system. A detailed explanation of this optimization problem is mentioned in section 4.

2.2. Resilience enhancement via operational strategies

Even though the grid is hardened with significant resources, it is essential to effectively operate the system to serve the emergency period's demand. To serve the demand during ERT, thereby to enhance the system resilience, here an operational strategy is formulated, and its procedure is discussed below:

- *Clustering of distribution network:* Following an earthquake, the distribution network groups into a '*k*' number of clusters to restore the supply for maximum possible consumers, including critical/priority-based. In other words, the formation of clusters leads to minimal overall load curtailment. Here we assume that the communication link is available between the control centre and HBIs during the event.
- *Optimal operation of ESUs:* Initially, the communication infrastructure derives the SOC level of HBIs to the control centre available within the cluster. The formulated optimization problem consists of the status of HBIs (i.e., its SOC level), the power demand of the critical/priority-based load, and the demand for domestic load within the clusters. Maximizing the overall energy served during the targeted emergency response time (ERT) using linear programming (LP) provides optimal operation of ESUs within the clusters.

The conceptual system performance to enhance system resiliency against natural disasters has been proposed in many literature studies [38,46,47]. Fig. 4 compares various resilience enhancement strategies and the proposed framework against the natural disaster using the distribution system performance. Here during the occurrence of an event at the time t_e, the system has begun to degrade and reached a minimum level at the time t_{r1}. Suppose the ESU planning for improving the grid flexibility considers the impact of a natural disaster; in that case, the interruption time will shift to t_{r2} by a factor of ΔT_1 and the system performance improves by ΔP_{D1}. It is also evident that, by considering the effect of HBI in the system, the interruption time and the system performance improves by ΔT_2 and ΔP_{D2}, respectively.

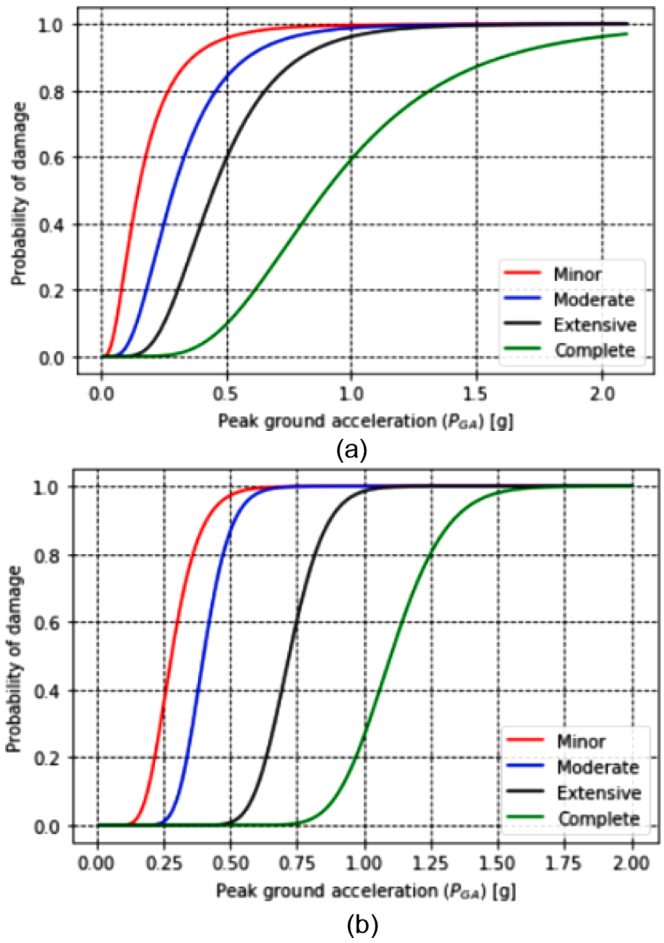

Fig. 5. The Fragility curves of (a) Electrical substation (b) Distribution lines.

3. Earthquake characterization and vulnerability assessment

3.1. Modelling seismic activity

The estimation of seismic hazard is essential for any infrastructure planner. The earthquake intensity varies from hypocenter to the point of a particular location due to attenuation. Experts accept that the soil type and geotechnical characteristics are significant factors for high ground acceleration during earthquakes. In general, regression analysis includes the parameters such as the intensity of the earthquake, distance from the surface (at the epicenter) to the hypocenter, commonly known as depth, and the distance between the equipment and the epicenter (fault location) represents the attenuation. A general regression model for attenuation is shown in (3) [42].

$$\ln(X) = c_0 + c_1F_1(R) + c_2F_2(D) + c_3F_3(M_w) \quad (3)$$

where X is the peak ground acceleration or spectral displacement in gals [g], R is the distance between the epicenter and the location of the equipment, D is the distance between the epicenter and the hypocenter, M_w is the moment magnitude, and c_0, c_1, c_2, & c_3 are regression coefficients.

3.2. Fragility model

The fragility model of equipment can be derived through various means such as (i) by experts' viewpoint, (ii) statistical models built from an extensive failure record database, (iii) experimental or simulation-based characterization of specific equipment under a series of shocks with various intensities, and (iv) mixed model by combining the above

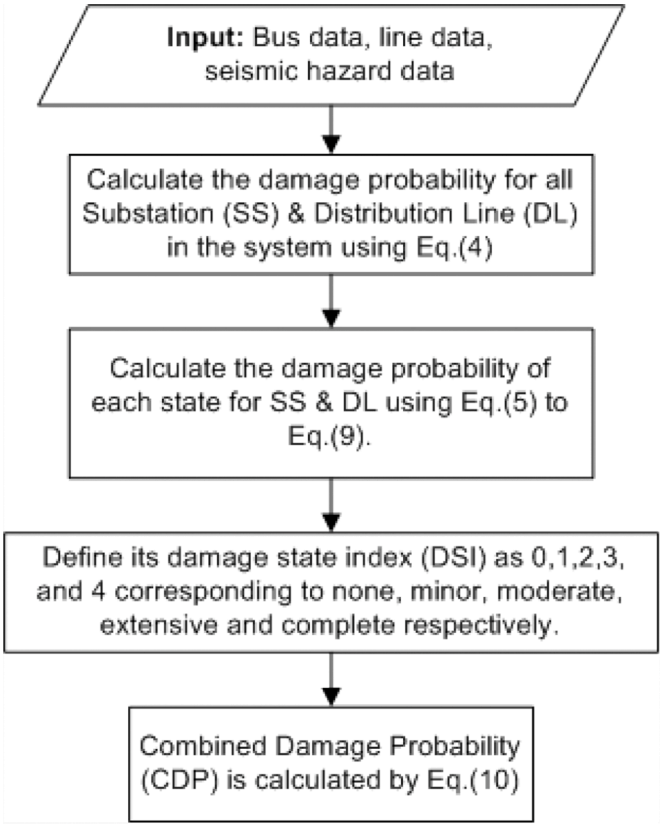

Fig. 6. Evaluation procedure of Combined Damage Probability.

methods [48]. This model's outcome provides the probability of failure of the equipment (*electrical infrastructure*) under the potential intensity of a disaster. For deriving a better solution, the various damage states defined in this paper are none, minor, moderate, extensive, and complete, depending on the seismic activity's intensity. For a given level of seismic activity (X), the lognormal fragility curves derive the level of damage reflecting the probability of attaining or surpassing a damaged state. The fragility curve corresponding to a damage state is defined by its median value of spectral displacement and lognormal standard deviation (β_{d_s}) [49]. Equation 4 represents the probability of attaining or surpassing a particular damage state (d_s).

$$P[d_s S_d] = \phi\left[\frac{1}{\beta_{d_s}}\ln\left(\frac{S_d}{\overline{S}_{d,d_s}}\right)\right] \tag{4}$$

where, S_d is the spectral displacement, $\overline{S}_{d,d_s}$ is the median value of spectral displacement, β_{d_s}, is the standard deviation of lognormal of spectral displacement for a damage state d_s, and ϕ is the standard normal cumulative distribution function. In this article, the fragility model derives the failure probability of both electrical substations and distribution lines. Its corresponding fragility curves are shown in Fig. 5(a) and Fig. 5(b), respectively.

3.3. Damage probability of electrical infrastructure

Since the ESU investment is high, the location chosen to install it must have a null or minimum impact due to natural disaster, or it must be more structurally stable to withstand the disaster (which may cater to an additional cost). Estimation of substation's unavailability due to the earthquake is equally vital as estimating the unavailability of overhead distribution lines that carry power to the end-users, the reason being that the large-scale ESUs connects the grid via substations. Henceforth, in this article, the combined fragility model of both substation and distribution lines is proposed, which quantifies the overall failure probability and its damage states such as none, minor, moderate, extensive, and complete. Equation (5) to (9) represents the cumulative probability of each damage state of substation (SS) and distribution lines (DL). Each state's damage probability is assessed by simplifying the equations (5) – (9). Equation (10) represents the combined cumulative damage probability, and the evaluation procedure of combined damage probability is shown in figure 6.

$$P(d_s = noX)_{SS|DL} = P_{no} + P_{mi} + P_{mo} + P_{ex} + P_{co} = 1 \tag{5}$$

$$P(d_s = miX)_{SS|DL} = P_{mi} + P_{mo} + P_{ex} + P_{co} \tag{6}$$

$$P(d_s = moX)_{SS|DL} = P_{mo} + P_{ex} + P_{co} \tag{7}$$

$$P(d_s = exX)_{SS|DL} = P_{ex} + P_{co} \tag{8}$$

$$P(d_s = coX)_{SS|DL} = P_{co} \tag{9}$$

$$CDP_j = P[d_s S_d]_{SSj} \;\&\; \{P[d_s S_d]_{DL1} | P[d_s S_d]_{DL2} \,|\cdots|\, P[d_s S_d]_{DLl}\} \tag{10}$$

where the subscripts *no, mi, mo, ex,* and *co* represents the damage state such as none, minor, moderate, extensive, and complete respectively; l is the number of distribution lines connected to the node j.

3.4. Monte-carlo based probabilistic earthquake hazard model

The occurrence of earthquakes at any location is purely a random event, and therefore modelling earthquakes using the probabilistic approach might be more realistic. For better infrastructure planning, it is essential to consider all the possible earthquake scenarios (within the chosen region) and therefore, a Monte-Carlo based probabilistic approach is developed in this paper to evaluate the vulnerability of substations and distribution lines. The procedure followed to develop this model is explained as follows:

Step 1: From the d seismic catalogue, parameters such as moment magnitude, location (latitude and longitude), and distance from the epicenter to the hypocenter are derived.
Step 2: Using the data derived in *step 1*, identify the best suitable distribution function to evaluate the parameters such as mean, standard deviation, and variance for the variables such as earthquake magnitudes, its location, and source to chosen site distance.
Step 3: Based on the statistical data obtained from *step 2* characterize the earthquake probability distribution function (PDF) for parameters such as earthquake magnitudes (M_w), its location (Loc) (Latitude and Longitude), source to chosen site distance (R). For instance, based on the historical seismic data for the selected region of study, the skewness and kurtosis measures are evaluated (which are within the range of -1 to 1), from which it is evident that the earthquake parameters can be modelled using normal distribution function as shown in (11), (12), and (13) respectively.

$$PDF_{M_w}(M_w) = \frac{1}{\sqrt{(2\pi)\sigma[M_w]}} \times e^{-(M_w - \mathrm{E}(M_w))/\sqrt{2\sigma[M_w]})^2} \tag{11}$$

$$PDF_{Loc}(Loc) = \frac{1}{\sqrt{(2\pi)\sigma[Loc]}} \times e^{-(Loc - \mathrm{E}(Loc))/\sqrt{2\sigma[Loc]})^2} \tag{12}$$

$$PDF_{R}(R) = \frac{1}{\sqrt{(2\pi)\sigma[R]}} \times e^{-(R - \mathrm{E}(R))/\sqrt{2\sigma[R]})^2} \tag{13}$$

Step 4: With the PDF for earthquake parameters, generate n number of possible earthquake scenarios for the chosen region using a Monte-Carlo based approach.
Step 5: The spectral displacement or PGA in gals [g] is evaluated with the outcomes of *step 4*.
Step 6: With PGA as input to the substations and distribution lines' fragility model, all possible failure likelihood of substations and distribution lines are evaluated.

4. Optimization problem

4.1. Three-dimensional hardening

The objective function consists of three components: cost for establishing ESUs, UCs, and communication infrastructure for HBIs as given in (14). The costs associated with ESUs are capital investment (which includes energy rating cost, power rating cost, and fixed installation cost), land required to install ESU and its allied cost, operation & maintenance cost of ESUs, and grid performance cost due to ESUs (which includes voltage deviation cost, line loading cost and cost of power loss) which are represented from (15) to (18). The costs associated with cabling are the capital investment of UCs (which includes cable cost per km, and its fixed cost) is represented in (19). The cost associated with HBIs is the capital investment of communication infrastructure for HBIs represented in (20). As mentioned earlier, the presence of HBI components may differ among load center. This aspect is reflected using the binary variables such as b_{BIS}, b_{PV}, and b_{EV} for BIS, standalone solar-rooftop, and electric vehicles, respectively in (20).

$$C_I^{ESU} = \sum_{i=1}^{N_{ESU}} \left[C_{PI}^{ESU} + C_{EI}^{ESU} + C_{FI}^{ESU} \right] \tag{15}$$

$$C_{land}^{ESU} = \sum_{i=1}^{N_{ESU}} C_{land}^{N_n} \times PS^{ESU} \ \forall \ N_n \tag{16}$$

$$C_{OM}^{ESU} = \sum_{i=1}^{N_{ESU}} \sum_{t=1}^{T} \left[P_{Sell,t} \times \mathbb{T}_{Sell,t} - P_{Pur,t} \times \mathbb{T}_{pur,t} \right] + C_F^{ESU} \times P_{rated}^{ESU} \tag{17}$$

$$C_{GP}^{ESU} = \sum_{n=1}^{N_n} \left| V_{target} - V_b^{ESU} \right| \times \mathfrak{C}_{VD} + \sum_{l=1}^{N_L} \%LL^{ESU} \times \mathfrak{C}_{LL} + \sqrt{\sum_{l=1}^{N_L} \left(P_{Loss,l}^2 + Q_{Loss,l}^2 \right)} \times \mathfrak{C}_{Loss} \tag{18}$$

$$C_I^{UC} = \sum_{i=1}^{N_{UC}} L_{UC,i} \times C_{pk}^{UC} \tag{19}$$

$$C_I^{HBI} = \sum_{i=1}^{N_{HBI}} b_{BIS} \times C_{ci}^{BIS} + b_{PV} \times C_{ci}^{PV} + b_{EV} \times C_{ci}^{EV} + C_{FI}^{HBI} \tag{20}$$

4.1.1. Optimization constraints

In the modern distribution system, the real and reactive power demand of general load, electric-vehicle, and HBI at any time t at i^{th} bus must be satisfied by the power from the REPs, the power absorbed or injected from ESUs, the power grid, and the power losses. This balance in real and reactive power is represented by (21) – (22). The operational constraints governing the real and reactive power flow is given by (23) – (24). When REPs and large-scale ESUs are integrated into the grid, its performance will be affected. To ensure this, limits of the node voltage and line loading (of already installed lines) are considered as given in (25) – (26).

$$P_D^{i,t} + P_{EV}^{i,t} + P_{HBI}^{i,t} = P_{PV}^{i,t} + P_{ESU}^{i,t} + P_{grid}^{i,t} + P_{loss}^{t} \ \forall \ t = 1, 2, \ldots, T \ \& \ i = 1, 2, \ldots, \ N_n \tag{21}$$

$$Q_D^{i,t} + Q_{EV}^{i,t} + Q_{HBI}^{i,t} = Q_{PV}^{i,t} + Q_{ESU}^{i,t} + Q_{grid}^{i,t} + Q_{loss}^{t} \ \forall \ t = 1, 2, \ldots, T \ \& \ i = 1, 2, \ldots, \ N_n \tag{22}$$

$$P_{flow}^{i,t} = \ V^{i,t} \times \sum_{i,j \in N_n} V^{j,t} \left(G_{ij} cos\theta_{ij,t} + B_{ij} sin\theta_{ij,t} \right) \tag{23}$$

$$Q_{flow}^{i,t} = \ V^{i,t} \times \sum_{i,j \in N_n} V^{j,t} \left(G_{ij} sin\theta_{ij,t} - B_{ij} cos\theta_{ij,t} \right) \tag{24}$$

$$V_{min} < V_t^n < V_{max} \ \forall \ n = \ 1, 2, \ldots, N_n \tag{25}$$

$$LL_t^l < LL_{max}^l \ \forall \ l = \ 1, 2, \ldots, N_L \tag{26}$$

The power absorbed or injected by ESUs depends on its mode of operation, such as charging or discharging. The SOC of ESU decides the mode of operation. Since this article's main objective is to operate ESUs under the emergency response period, only discharging mode is shown. Therefore, the constraints corresponding to ESUs are limits of discharging power and energy from ESUs, limits of SOC of ESUs, and apparent power, which is given by (27) – (30). As mentioned earlier, UCs are installed to increase the possibility of load connectivity during the emergency response period. Therefore, it is essential to consider the loading capacity of UCs as given by (31). Apart from all the technical constraints, budget allocation for hardening is the major constraint which is given by (32).

$$P_{min}^{ESU} < P_t^{ESU} < P_{max}^{ESU} \ \forall \ t = \ 1, 2, 3, \ldots\ldots, T \tag{27}$$

$$E_{min}^{ESU} < E_t^{ESU} < E_{max}^{ESU} \ \forall \ t = \ 1, 2, 3, \ldots\ldots, T \tag{28}$$

$$SOC_{min}^{ESU} \leq SOC_t^{ESU} \leq SOC_{max}^{ESU} \tag{29}$$

$$S^{ESU} = \sqrt{P_{ESU}^2 + Q_{ESU}^2} \tag{30}$$

$$LL_t^{UC} < LL_{max}^{UC} \ \forall \ UC = \ 1, 2, \ldots, N_{UC} \tag{31}$$

$$C_I^{ESU} + C_I^{UC} + C_I^{HBI} \leq Budget_{max} \tag{32}$$

4.2. Optimal ESU operation during ERT

Following an event (or disaster), the system's performance degrades, as shown in figure 4. As mentioned earlier, it is assumed that the communication link between the control center and HBIs is in operation during ERT through which the SOC of HBIs across the distribution system is derived. To improve the system performance during ERT, it is essential to maximize the resiliency index (RI), defined as the ratio of energy served during ERT to the expected energy demand. For the maximum value of RI within the cluster during ERT, it is essential to find the optimal power output from ESU for the given SOC level of HBIs (distributed within the cluster). Maximizing the objective function given by (33) constrained with (34) to (39) using LP provides the optimal power output of ESU during ERT. In equation (33), the difference between t_e and t_{r_3} given the value of ERT.

$$RI = \ \sum_{t=t_e}^{t_{r_3}} \left(P_{D,t}^{C|P,k} + P_{D,t}^{do,k} \right) \Big/ P_{D,t}^{Exp,k} \ \forall \ k \tag{33}$$

$$P_{D,t}^{C/P,k} + P_{D,t}^{do,k} = P_t^{ESU} + P_t^{HBI} \ \forall \ t = 1, 2, 3, \ldots, E_t \tag{34}$$

$$\sum_{t=t_r}^{t_{r_3}} P_t^{ESU} \leq E_D^{C|P} \tag{35}$$

$$\sum_{t=t_r}^{t_{r_3}} P_t^{ESU} * \Delta t \leq E_{max}^{ESU} \tag{36}$$

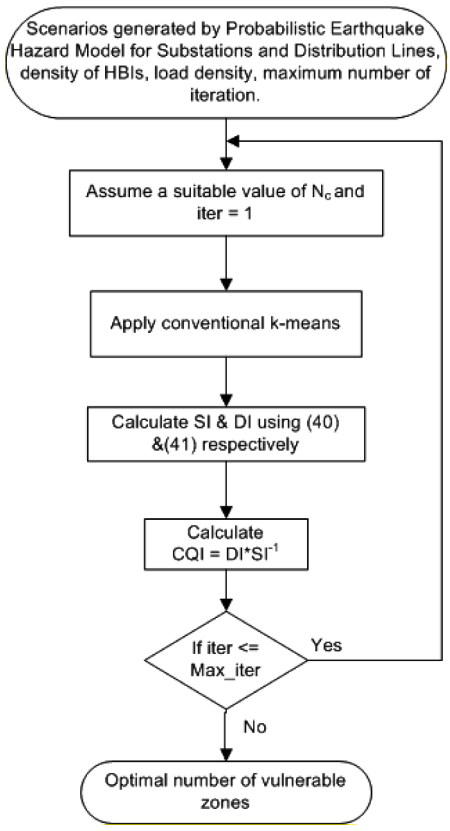

Fig. 7. Flowchart of clustering methodology for Optimal vulnerable zones.

$$SOC_{min}^{ESU} \leq SOC_{t}^{ESU} \leq SOC_{max}^{ESU} \tag{37}$$

$$0 \leq P_{t}^{ESU} \leq P_{max}^{ESU} \tag{38}$$

$$0 \leq E_{t}^{ESU} \leq E_{max}^{ESU} \tag{39}$$

where, $P_{D,t}^{C/P,k}$ and $P_{D,t}^{do,k}$represents the power demand of critical/priority-based load and domestic load in kth cluster respectively at time t, $E_{D}^{C|P}$ represents the expected energy demand from a critical/priority-based load during the emergency period (E_t), P_{t}^{ESU} represents the power output from ESU at time t, E_{t}^{ESU} represents the energy demand satisfied by ESU at time t, and P_{t}^{HBI} represents the power output from HBI at time t.

5. Proposed methodology

The problem formulated in this article includes both grid-side and demand-side hardening to enhance the overall system performance during the emergency period. Hardening of a network comes under planning activity; therefore, the distribution system modelled in this study includes the uncertainty of REPs and load (as mentioned in section 2) [40]. A bi-level approach is proposed to solve the formulated optimization problem. In the first level, optimal clusters reflecting the possible vulnerable zones of the distribution network are identified. In the second level, the objective function given by (14) is minimized constrained with (21) – (32) using the hybrid algorithm.

5.1. First level optimization

The utilities' main objective is to ensure the power supply for all the loads during both normal and extreme conditions. However, there are many practical challenges faced by the utilities to supply power during extreme conditions. The utilities can streamline these challenges if the vulnerable zones of the distribution network are identified. Also, these challenges may vary across the distribution network, depending on load density. Therefore, to identify the vulnerable zones, the distribution network is clustered based on the probabilistic earthquake hazard model's outcome, the density of HBIs, and load density using the *k-means* algorithm. Since the number of clusters is provided as an input for the k-means algorithm, a methodology based on the Silhouette index (SI) and Davies Bouldin index (DI) given in (40) and (41) respectively is applied to find the optimal number of clusters. The flowchart of the clustering methodology is shown in Fig. 7.

$$SI = \frac{1}{N_{tot}} \sum_{i=1}^{N_{tot}} \left(\frac{1}{N_C} \sum_{j=1}^{N_c} S(j) \right) \tag{40}$$

$$DBI = \frac{1}{N_{tot}} \sum_{i=1}^{N_{tot}} \underset{i \neq j}{max} \left(\frac{X(i) + X(j)}{d_{ij}} \right) \tag{41}$$

where N_{tot} is the total number of nodes in a given set, N_c is the number of clusters and $S(j)$ represents the ratio of the difference between the minimum average distance and the average distance between j^{th} node and all other nodes to the maximum of both, $X(i)$ and $X(j)$ are the average distance between each location of cluster i & j and centroid of that cluster respectively, d_{ij} is the distance between the centroids of cluster i and cluster j.

5.2. Second level optimization

In this section, the proposed methodology to optimize the overall hardening is discussed. The flowchart of the proposed methodology is shown in Fig. 8. Here, the set of buses/nodes and distribution lines that belong to the optimization algorithm's search space is derived using Algorithm – I. Here, the nodes for set {B} are chosen to not fall on the vulnerable zones. The distribution lines for set {L} is chosen based on step 8 and step 9 of the *Algorithm – I* discussed below. In this algorithm, the distance matrix API is imported from cloud service to calculate the distance between the given two nodes (represented by CS_{dis}). Here in the expression of CS_{dis}, OH_{dis}^{l} represents the distance of overhead line l, the parameters d and m are constants whose value depends on the line loading and budget. Generally, the effect of earthquakes on substations and distribution lines is calculated based on PGA and for the underground cables, it is computed using peak ground velocity (PGV). The expression for PGV applied in this article is given by (42) [50]. The worst-case PGV mentioned in Fig. 8 is obtained by calculating PGV for the worst earthquake magnitude.

$$\ln(PGV) = \begin{cases} -0.6615 + 0.3463 \times M_w - 0.0262 \times R - 0.0021 \times D \; firm \; soil \\ -1.1646 + 0.4299 \times M_w - 0.0159 \times R - 0.003 \times D \; soft \; soil \\ -0.7649 + 0.3729 \times M_w - 0.0229 \times R - 0.0044 \times D \; soil \end{cases} \tag{42}$$

6. Results of numerical experiments

The system considered in this study for optimal hardening is the 156-bus power distribution system of Dehradun district, Uttarakhand, India, which comes under seismic zone IV. Based on the chosen region's seismic catalogue, the moment magnitude of the earthquake ranges between $3.5 \leq M_w \leq 5.3$ and the equation (43) represents its corresponding regression model [42,51].

$$\ln(PGA) = c_0 + c_1 ln(R) + c_2 M_w - c_3 ln(R + 15) \tag{43}$$

The value of seismic regression coefficients c_0, c_1, c_2, c_3 considered in this study are 2.29, 1.95, 2.07, and 4.03, respectively. Here, the Na-S battery technology is chosen for ESU because it has the least climatic impact of 30 kg CO2-eq/kWh [52]. Additional input parameters considered in this study are shown in Table 1. In this table, the Time of

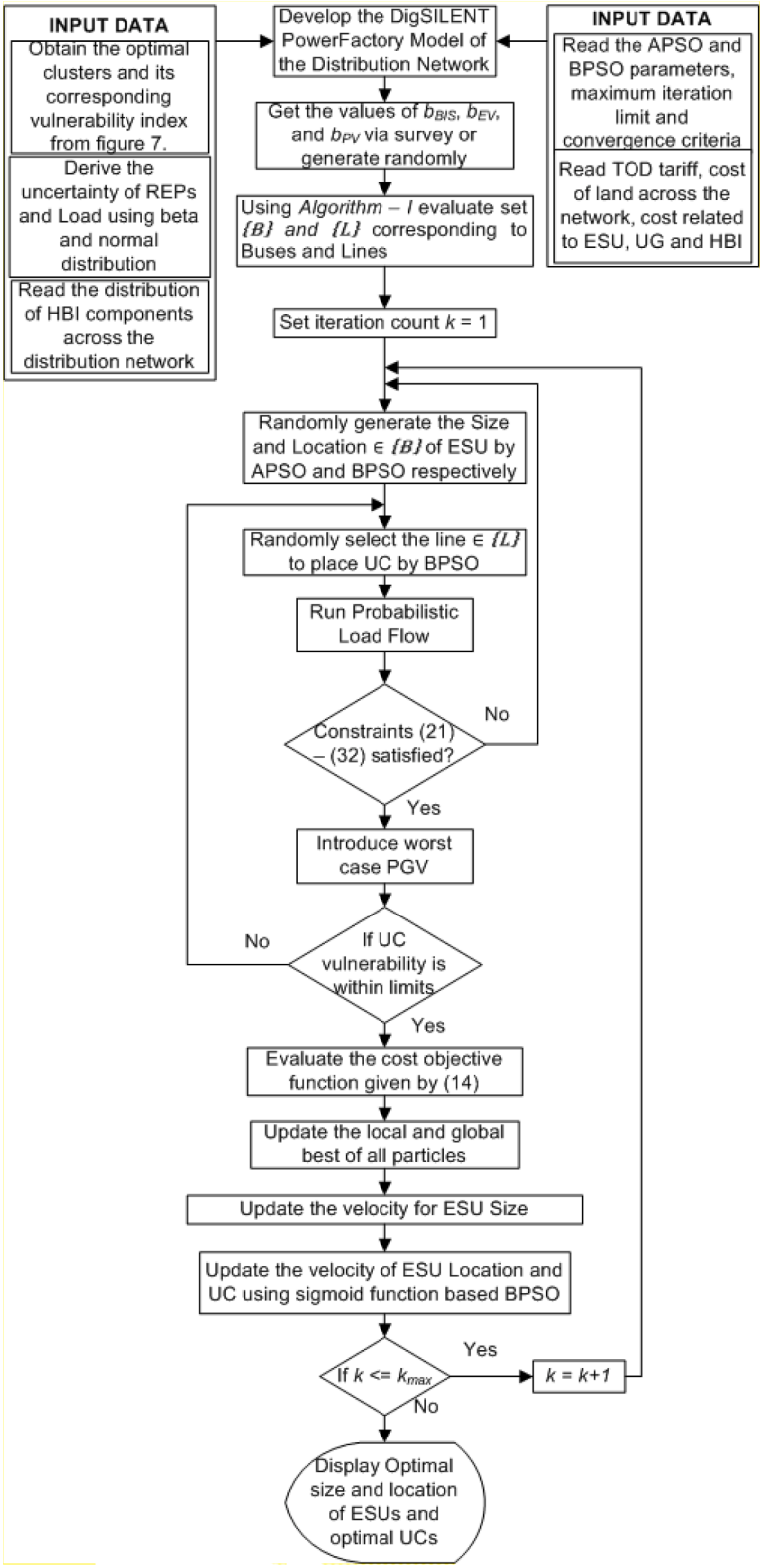

Fig. 8. Flowchart of Proposed Methodology.

Day (TOD) and its corresponding tariff is obtained from [53]. Table 2 shows the predicted critical/priority-based load (hospitals, water pump houses, VIP/VVIP) across the distribution system. Table 3 shows the median and lognormal standard deviation of the fragility curves corresponding to the different damage states considered in this study [49]. These days, the presence of BIS across the distribution system is significant. However, solar PV rooftop and electric vehicles across the distribution system are significantly less compared to BIS. Therefore, this study is performed by considering two schemes. The first scheme considers only BIS (modelled as HBI with $b_{PV} = b_{EV} = 0$), and the second scheme considers HBI (consisting of BIS, solar PV rooftop and electric vehicles) as a part of the demand-side strategy. The results

Table 1
Input Parameters for Optimal Hardening.

Time of Day & Tariff		
Summer	*April – September*	
Off-peak	12 AM – 7AM	0.065$/unit
Normal	7AM – 6PM	0.081$/unit
Evening Peak	6PM – 11PM	0.11$/unit
Off-peak	11 PM – 12AM	0.065$/unit
Winter	*October – March*	
Off-peak	12AM – 6AM	0.065$/unit
Morning Peak	6AM – 9AM	0.11$/unit
Normal	9AM – 6PM	0.081$/unit
Evening Peak	6PM – 10PM	0.11$/unit
Off-peak	10PM – 12AM	0.065$/unit

Earthquake parameters			
	Mean	*SD*	*Variance*
M_w	3.645349	0.761215	0.579449
Location	30.165N, 80.004E	0.761536,1.511734	0.579937, 2.285339

Parameters for Optimization	
C_{ipk}^{UC}	46725$/km
C_{ci}^{BIS}	50$/BIS
C_{ci}^{PV}	150$/PV
C_{ci}^{EV}	100$/EV
$\mathfrak{S}_{env}$	0.0085 $/kg CO2
$\mathfrak{S}_{VD}$	0.142 in $/p.u
$\mathfrak{S}_{LL}$	0.503 in $/p.u
$\mathfrak{S}_{Loss}$	0.265 in $/p.u
$[V_{min}, V_{max}]$	[0.95 p.u, 1.05 p.u]
LL_{max}^{l}	80% of line capacity

Table 2
Predicted Peak Values of Critical/Priority-Based Loads.

Location	Load in MVA	Location	Load in MVA
Anarwala	0.3964	Govindgarh	0.6442
Araghar	3.3698	HimalayanHospital	0.9911
Bhaniyawala	0.7434	Jollygrant	0.5451
Bindal	0.8672	Kunjbhavan	1.4867
Dakpatti	1.9822	Natraj	0.0991

Table 3
Median and β_{d_s} Values of Electrical Infrastructures for Different Damage States.

Electrical Infrastructure	Damage State	Median [g]	β_{d_s}
Substation	Minor	0.15	0.7
	Moderate	0.29	0.55
	Extensive	0.45	0.45
	Complete	0.9	0.45
Distribution Lines	Minor	0.28	0.3
	Moderate	0.4	0.2
	Extensive	0.72	0.15
	Complete	1.1	0.15

obtained from these schemes are discussed further.

6.1. Results of first scheme

As mentioned earlier, in this scheme, the demand-side strategy applies only BIS. From the survey conducted across the system, 60% of domestic load center have installed a local backup using BIS. Therefore, it is essential to introduce the BIS model into the distribution system model. The normal distribution function given by (44) represents the uncertainty introduced by the presence of BIS (rated between 600 VA to 1150 VA) during the planning horizon (of 10 years) in this scheme.

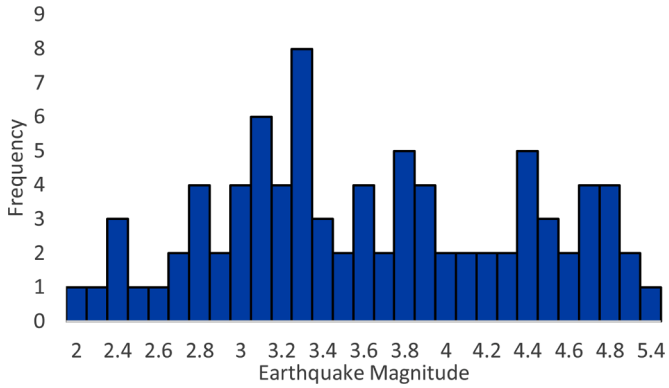

Fig. 9. Normalized Occurrence frequency of Earthquakes in the region of study.

$$PDF_{BIS}(P_{BIS}) = \frac{1}{\sqrt{(2\pi)}\sigma[P_{BIS}]} \times e^{-\left(P_{BIS}-\mathrm{E}(P_{BIS})/\sqrt{2\sigma[P_{BIS}]}\right)^2} \quad (44)$$

In this scheme, the cases considered to study the proposed framework are case *A:* worst-case seismic faults and case *B:* the most frequent seismic fault in the region. Here, based on equation (45) (derived from the seismic study performed in the chosen region [42]), and the normalized (by a factor 100) frequency of occurrence data (for the past five years) shown in Fig. 9 (representing the historical catalog of seismic activity), it is evident that the most frequent seismic fault in the chosen region is of moment magnitude 3.3. The frequent earthquake of moment magnitude 3.3 occurs in eight different locations across the region of study.

$$Log_{10}N = 5.7 - 0.71M \quad (45)$$

where M is the moment magnitude of the earthquake and N is the number of earthquakes with moment magnitude M. Based on the historical seismic catalogue, the seismic fault that occurred in the location (30.45°N 77.92°E) with a moment magnitude of 5.4 is the worst-case seismic fault stricken in the region of study. As described in Section 5, the *Algorithm - I,* based on the vulnerability assessment (described in Section 3), the set of nodes and distribution lines for ESU placement are derived. The accessible substations and distribution lines after the worst seismic fault are obtained, shown in Table 4 and Table 5, respectively (for *case A*). Followed by the most frequent earthquakes analyzed for all eight different locations in the study region, all substations and distribution lines are accessible as per the *Algorithm - I*. Therefore, for the chosen system, identifying the optimal solution for *case B* is like ESU planning for normal conditions.

Having the accessible substations and distribution lines, the objective function is given by (14) (considering $b_{PV} = b_{EV} = 0$) constrained with (21) – (32) derives the optimal size and location of ESUs, which can improve the grid flexibility during the normal condition and the system resiliency during the emergency condition. The results of the optimal solution shown in Table 6 reflect the global minima obtained using an algorithm that combines APSO and BPSO [40]. During normal conditions, the optimal ESU improves the bus voltage profile of the distribution system. This is evident from Fig. 10, which represents the percentage comparison of bus voltage profile for cases with and without ESUs. Here the x-axis represents the buses in the system and y-axis represents the difference in voltage magnitude (in p.u.) with and without ESU in percentage.

As mentioned earlier, the objective function (34) constrained with (35) – (40) (by considering P_t^{BIS} in place of HBI in (35)) solved using LP derives the optimal operation of ESUs within the cluster by assuming two SOC levels for BIS such as 0% and 100%. Fig. 11 shows the maximized value of RI by the optimal operation of ESUs along with BIS for

Table 4
Accessible Distribution Lines Followed by Worst Case Seismic Fault: for the first scheme.

LineSection	DamageProbability	DSI_{DL}	LineSection	DamageProbability	DSI_{DL}	LineSection	DamageProbability	DSI_{DL}
L08	0.5114	1	L42	0.6010	3	L66	0.6460	0
L09	0.8922	0	L48	0.7887	2	L67	0.8006	0
L10	0.5156	1	L49	0.9027	2	L68	0.8673	2
L11	0.8975	0	L56	0.6258	3	L69	0.8004	0
L12	0.5213	2	L57	0.6258	3	L70	0.8409	0
L19	0.6428	3	L60	0.6411	3	L72	0.5024	3
L20	0.5558	3	L61	0.6411	3	L73	0.6601	0
L32	0.5401	1	L63	0.5213	3	L75	0.5878	3
L33	0.5293	1	L64	0.7461	2	L76	0.5932	3
L34	0.4371	2	L65	0.8338	0			

Table 5
Accessible Substations Followed by Worst Case Seismic Fault: for First Scheme.

Substation	Damage Probability	DSI_{SS}	Substation	Damage Probability	DSI_{SS}	Substation	Damage Probability	DSI_{SS}
Araghar	0.488396	3	Lachiwala	0.486559	3	Ramnagar Danda	0.11555	2
Bairaj	0.331563	1	Lakhamandal	0.346177	3	Rishikesh	0.302965	1
Bhaniyawala	0.107374	2	Laltapper	0.179293	1	Savra	0.167859	2
Bhoopatwala	0.378232	1	ManeriBhali	0.293203	1	ShantiKunj	0.349822	1
Doiwala	0.103981	2	Nagarpalika	0.292999	1	Transport Nagar	0.479541	3
Himalayan Hospital	0.112021	2	Raiwala	0.340927	1	Tuini	0.339201	1
Jollygrant	0.128834	2						

Table 6
Optimal Results of Distribution System Hardening: for First Scheme.

No of ESUs	Location Name	Lat(°N)	Lon(°E)	Size of ESU	Optimal value of Objective Function
14	Bhaniya wala	30.3657	78.0445	0.5601	442388953.234594
	Bhoopat wala	30.3069	78.0499	1.1191	
	Jollygrant	30.3305	78.0297	0.6001	
	Lachiwala	30.3916	78.0944	0.9977	
	Lakha mandal	30.3015	78.0583	1.0158	
	Laltapper	30.4555	78.1023	0.6393	
	Maneri Bhali	30.2670	78.0909	0.9557	
	Nagar palika	30.1064	78.2815	1.6935	
	Raipur	30.5721	77.9721	1.6228	
	Ramnagar Danda	30.2967	78.0141	1.9725	
	ShantiKunj	30.3090	78.0948	0.5136	
	Transport Nagar	30.0222	78.2147	1.2547	
	Bhaniya wala	30.3927	77.8096	0.9243	
	Bhoopat wala	30.8223	77.8546	1.1330	

various targeted ERTs.

6.2. Results of second scheme

In the second scheme, the proposed demand-side resiliency enhancement strategy applies HBI. As mentioned earlier, the outcome of the survey across the system shows that the BIS is installed in about 60% of the domestic load center. Here, the BIS's presence is modelled similar to the first scheme. A similar distribution function is followed for the presence of solar PV rooftop and electric vehicles with a capacity of (3×10) kWp and 30kW, respectively in the distribution system model of DigSILENT PowerFactory. With the input data mentioned from Table 1 to Table 3, the proposed bi-level approach is applied to obtain the optimal hardening solution. After getting the optimal hardening, this scheme's effectiveness during the extreme condition (i.e., the worst-case seismic fault mentioned above) is tested for two cases. *Case I*: by considering the complete load connected to the system, and *Case II*: by considering only the critical loads of the system (mentioned in Table 2).

As discussed in section 5, the distribution network is clustered to obtain its vulnerable zones. The major components of the distribution network considered in this study are substations and distribution lines. Here the vulnerability of buses/nodes (substations) and the distribution lines are derived using the Monte-Carlo earthquake hazard model, as explained in section 3. Since the fragility of substations and distribution lines are different for the same earthquake activity [49], individual clustering of substations and distribution lines is performed. However, the combined damage probability is derived using (10). Using the clustering methodology mentioned in figure 7, the optimal number of vulnerable zones are obtained for substations and distribution lines. Fig. 12 and Figure 13, show that the optimal number of clusters for substations and distribution lines are two and four respectively. The optimal number of vulnerability zones and the possibility of risk are shown in Table 7.

Applying the *Algorithm – I*, twenty and thirty-one number of buses/nodes and distribution lines is obtained for *{B}* and *{L}* respectively shown in figure 14. In this figure, the substations and the distribution lines in the set *{B}* and *{L}* are represented by a red circle and red lines, respectively. With the derived input data for second-level optimization, the optimized cost of (14) obtained is 508847398.68 dollars. The optimal size and location of ESUs are shown in Table 8, and the optimal location of UCs is shown in Table 9.

During the normal condition, placing the ESUs at optimal locations with optimal size has significantly improved the bus voltage profile. The same can be evident from Fig. 15, which shows the percentage comparison of bus voltage profile cases with and without ESUs. Here the x-axis represents the buses in the system, and the y-axis represents the difference in voltage magnitude (in p.u) with and without ESU in percentage. Resiliency index (RI) is defined to measure the overall system performance for both cases I & II during the emergency period given by (33).

6.2.1. Case I

In this case, the value of RI is calculated using (33) by considering the complete load connected to the distribution system. Table 10 representing the RI values for various conditions such as without hardening, with only ESUs, and the proposed methodology shows the proposed

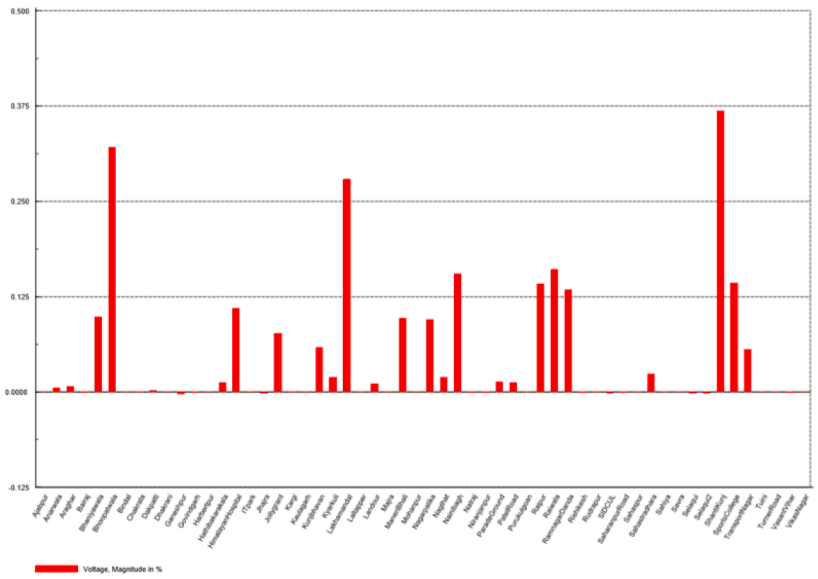

Fig. 10. Bus Voltage Profile Comparison - with and without ESU in percentage: for First Scheme.

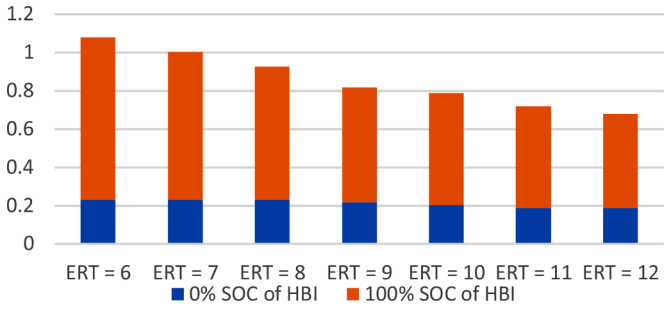

Fig. 11. Resiliency Index for Various SOC levels of HBI: for First Scheme.

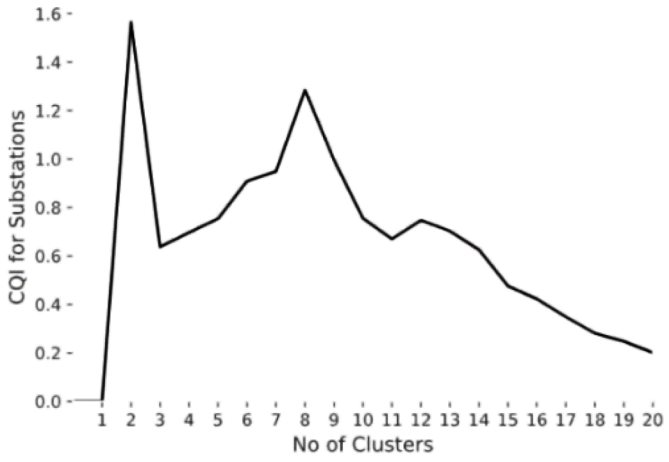

Fig. 12. Cluster Quality Index of Substation for different number of clusters.

framework's effectiveness. From this, it is evident that the proposed method has improved the overall energy served by three times of the case without any hardening measures and 1.5 times of the case with only ESUs.

6.2.2. Case II

Considering only the critical loads of the distribution system, as mentioned in Table 2, RI is calculated using (33) against various

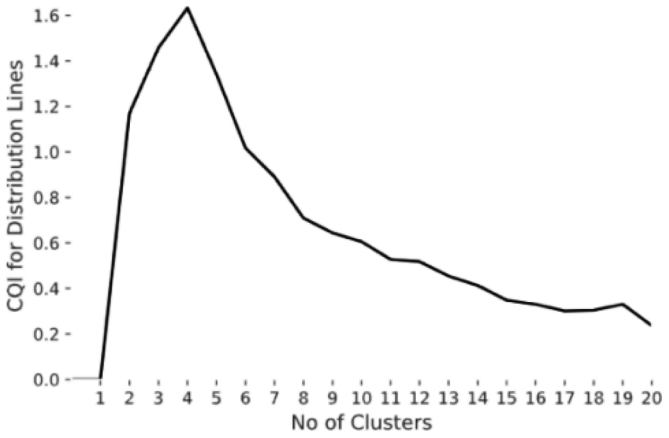

Fig. 13. Cluster Quality Index of Distribution Lines for different number of clusters.

Table 7
Optimal Clusters and its risk possibility of Substations and Distribution Lines.

Substations	**Optimal Clusters = 2**			
Possibility of Risk	*Cluster 1* High		*Cluster 2* Low	
Distribution Lines	**Optimal Clusters = 4**			
Possibility of Risk	*Cluster 0* High	*Cluster 1* Nil	*Cluster 2* Medium	*Cluster 3* Low

targeted ERT. A comparison is made with RIs for various conditions such as, with only ESUs and with the proposed methodology shown in Table 11. From this, it is apparent that the proposed method has significantly improved the energy served during the emergency period.

The obtained hardening results can improve the overall system performance during normal conditions. The results obtained for both cases I & II, show the proposed methodology can effectively improve the energy served during the emergency condition.

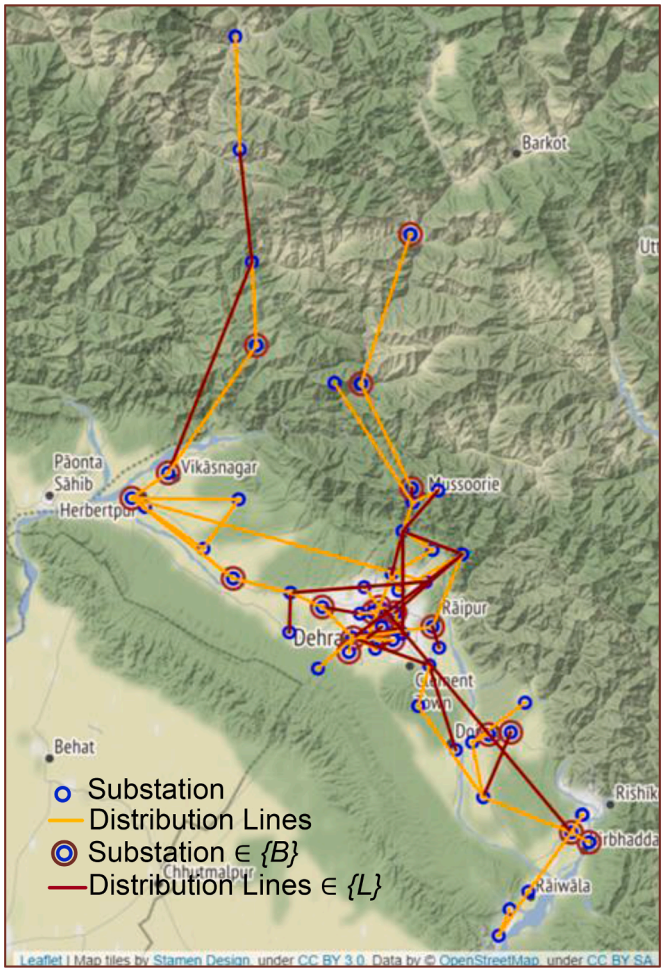

Fig. 14. Set of Substations and Distribution Lines derived from Algorithm – I.

Table 8
Optimal Size and Location of ESUs: for Second Scheme.

Optimal Number of ESUs	Location			Size in MVA
	Latitude	*Longitude*	*MSL*	
5	30.448	77.7195	439	1.3848
	30.3306	77.9574	610	1.1914
	30.30925	78.031806	640	1.5593
	30.6115	77.8753	1049	0.7573
	30.2811	77.9903	601	0.7208

7. Discussions

This section elaborates the proposed hardening strategy's effectiveness by comparing the system performance among various strategies (as mentioned in figure 4), such as without ESUs, with only ESUs and the proposed framework. As mentioned earlier, the PSO algorithm is better suitable for solving similar optimization problems [39]. To demonstrate the effectiveness of the hybrid algorithm (based on PSO), a comparison with algorithms like genetic algorithm (GA) and Ant Colony Optimization (ACO) based on parameters such as overall cost for utilities in dollars, optimal number of ESUs and UCs for both the schemes is shown in Table 12. Besides, other critical findings of this study are articulated in this section. Section 6 presents the results of numerical experiments for both schemes. The system chosen for this study is situated on a mixed terrain (situated on both hilly and plain region) comprises fifty-nine 33kV nodes and seventy-six 33kV lines. From the results of the first scheme, it is evident that, for *case A* (worst case scenario), out of fifty-nine nodes, only nineteen nodes and out of seventy-six lines, only twenty-nine lines are accessible (shown in figure 1) whereas, for *case B*, all nodes and lines are accessible. Therefore, any framework which applies to the normal condition is suitable for *case B*. However, the results obtained for *case A* proves that the system may not withstand a high impact low probability (HILP) seismic hazard, i.e., the worst seismic hazard.

Table 9
Optimal location of UCs.

Optimal No of UCs	From Bus	To Bus	Cluster	Distance in km
16	Anarwala	Hathibakarakala	2	5.3
	Bindal	Anarwala	2	6.7
	Bindal	Kaulagarh	2	4.8
	Bindal	Niranjanpur	2	8.2
	Bhaniyawala	HimalayanHospital	2	2.7
	Bhoopatwala	ShantiKunj	3	5.5
	Dhakrani	Harbertpur	3	2.8
	Dhakrani	VikasNagar	3	8.2
	Jhajra	Selaqui	2	7.8
	Laltapper	Bhaniyawala	0	7.4
	Majra	Mohanpur	0	11.1
	Majra	Niranjanpur	2	3.6
	Majra	TransportNagar	2	2.4
	Rishikesh	Laltapper	2	24.9
	Rishikesh	ManeriBhali	0	7
	Rishikesh	Raiwala	0	10.4

From figure 10, it is apparent that ESU placement obtained for *case A* also improves the bus voltage profile of the system during normal conditions. For any resilience enhancement framework, it is essential to minimize the load curtailment during ERT. Maximizing (33) constrained with (34) - (39) effectively utilizes the presence of HBIs (here, $b_{EV} = b_{PV} = 0$) to channelize ESUs, thereby to meet the overall demand with minimal load curtailment.

Fig. 11 shows that having 0% SOC of HBI (or without HBI), and the ESUs can satisfy approximately 20% of the identified critical/priority-based loads for all targeted ERT, however, having 100% SOC of HBI (i.e., with HBI) and the ESUs can satisfy approximately 50% to 80% of the identified load for ERT ranging six to twelve hours. This contribution of HBI directly decreases the initial investment of ESUs for utilities.

From results obtained for case I of the second scheme, it is evident that the overall system performance during ERT is increased approximately by 60% compared to without any hardening measures and by 33% with only ESUs. The results obtained for case II of this scheme indicate that the overall average system performance during targeted ERT increases by 80% compared to without any hardening measures and by 65% with only ESUs. Fig. 16 shows the comparison of RIs for various resilience enhancement strategies. Apart from increasing the energy served during ERT, the proposed framework decreases the cost of investment and operation & maintenance cost three times compared to a scenario with only ESUs as evident from Table 13.

8. Conclusion

The existing methods to enhance system resilience focuses only on grid-side solutions like capacity addition of resources which might increase the capital investment for utilities towards distribution system hardening. Sometimes, to improve system resilience via grid-side solution, the available resources like REPs and ESUs are utilized to form microgrids by placing sectionalizer switches at optimal nodes. However, these resources may fail to supply the demand during ERT because of its vulnerability towards disaster. In ESU planning, the existing methodologies consider the vulnerability of distribution lines ignoring the substations to which it is connected. However, to satisfy the demand during ERT, both the substations and distribution lines must operate. As an essential step in planning, it is required to consider all possible

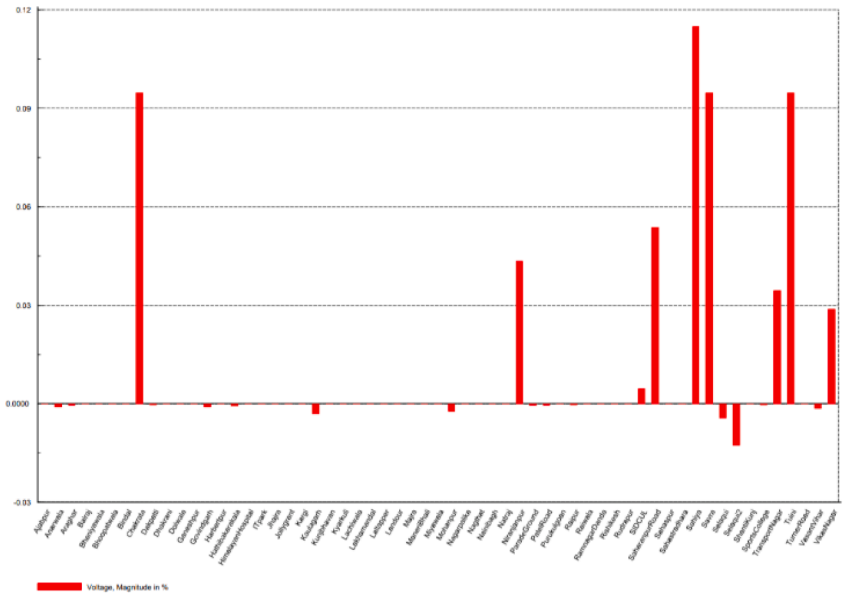

Fig. 15. Bus Voltage Profile Comparison - with and without ESU in percentage: for Second Scheme.

Table 10
Comparison of Resiliency Index for Case I.

Resiliency Index (RI)	Without hardening	Only ESU	Proposed Hardening
	0.0659	0.1258	0.1887

Table 11
Comparison of Resiliency Index for Case II.

Emergency Response Time	Resiliency Index (RI With only ESU	Proposed Hardening
8	0.2335	0.6935
9	0.2179	0.6013
10	0.2024	0.5857
11	0.1868	0.5318
12	0.1664	0.4935

earthquake occurrences over the chosen region. Therefore, this paper proposes an optimal planning methodology for distribution system hardening with the Monte-Carlo based probabilistic earthquake hazard model. Besides, the distribution system is clustered into vulnerable zones that can rationalize the utilities' challenges to supply the demand during emergency conditions, thereby providing realistic outcome from this probabilistic model.

With the increase in natural disasters and the smart grid's continuous evolution, the involvement of HBIs will undoubtedly play a vital role in developing a resilient grid. Therefore, this article proposes a resilience enhancement framework that combines both grid-side and demand-side strategies. The obtained results show that the capital investment towards the hardening of the distribution system can be decreased while increasing the energy served during ERT by three times.

The presented work mainly focuses on hardening strategies to enhance distribution system resilience against earthquake by combining grid-side and demand-side management strategies. Further directions to the presented study could be modelling of multiple disasters scenarios and developing various strategies to enhance system resilience.

CRediT authorship contribution statement

Balaji Venkateswaran V: Conceptualization, Methodology, Formal

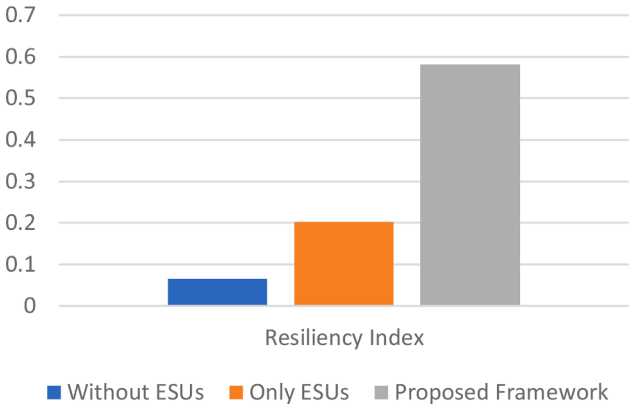

Fig. 16. Comparison of RI for various resilience enhancement strategies.

Table 13
Cost comparison with only ESUs and with ESU & HBI.

	Cost of Investment ($)	Cost of O&M ($)
Only ESUs	24624626.57	249363.3
ESU & HBI	7110995.4	72010.08

Table 12
Performance comparison of Hybrid Algorithm.

Algorithms	First Scheme Optimal ESUs	Costing for Utilities ($)	Second Scheme Optimal ESUs	Optimal UCs	Costing for Utilities ($)
GA	15	476171861.7	7	17	603446583.8
ACO	17	573715185.5	9	20	696444082.7
Hybrid Algorithm	14	442388953.2	5	16	508847398.7

Algorithm – I
Selection of Set of buses/nodes and lines.

Input: Vulnerable zones and its index of the network, N_n, N_L and location of substations and lines (i.e., latitude, longitude and mean sea level)

for $n = 1$ *to* N_n:
if i does not fall under the vulnerable zone:
$n \in \{B\}$
end for
for $l = 1$ *to* N_L:
if l falls under vulnerable zone:
if $((OH^{l}_{dis} - CS_{dis}) \ll d)$ && $((MSL_{fnode} - MSL_{tnode}) \ll m)$:
$l \in \{L\}$
end for

analysis, Software, Validation, Visualization, Writing – original draft. **Devender Kumar Saini:** Methodology, Investigation, Data curtion, Writing – review & editing. **Madhu Sharma:** Supervision.

Declaration of Competing Interest

The authors declare that they have no known competing for financial interests or personal relationships that could have appeared to influence the work reported in this paper.

Acknowledgment

The authors would like to thank DigSILENT, Germany for sponsoring the license of the PowerFactory software under PF4T scheme.

References

[1] Carpinelli G, Celli G, Mocci S, Mottola F, Pilo F, Proto D. Optimal Integration of Distributed Energy Storage Devices in Smart Grids. IEEE Trans Smart Grid 2013;4:985–95. https://doi.org/10.1109/TSG.2012.2231100.
[2] Jayasekara N, Wolfs P, Masoum MAS. An optimal management strategy for distributed storages in distribution networks with high penetrations of PV. Electr Power Syst Res 2014;116:147–57. https://doi.org/10.1016/j.epsr.2014.05.010.
[3] Nazaripouya H, Wang Y, Chu P, Pota HR, Gadh R. Optimal sizing and placement of battery energy storage in distribution system based on solar size for voltage regulation. IEEE Power Energy Soc. Gen. Meet. 2015. https://doi.org/10.1109/PESGM.2015.7286059.
[4] Senkel A, Bode C, Schmitz G. Quantification of the resilience of integrated energy systems using dynamic simation. Reliab Eng Syst Saf 2021;209. https://doi.org/10.1016/j.ress.2021.107447.
[5] TPDDL. 10 MW energy storage system at Tata Power Delhi Distribution's Rohini Substation n.d. https://www.tatapower.com/media/PressReleaseDetails/1617 (accessed January 12, 2020).
[6] Celli G, Mocci S, Pilo F, Loddo M. Optimal integration of energy storage in distribution networks. In: 2009 IEEE Bucharest PowerTech Innov Ideas Towar Electr Grid Futur; 2009. p. 1–7. https://doi.org/10.1109/PTC.2009.5282268.
[7] Qing Zhong, Nanhua Yu, Xiaoping Zhang, You Y, Liu D. Optimal siting & sizing of battery energy storage system in active distribution network. In: IEEE PES ISGT Eur. 2013. IEEE; 2013. p. 1–5. https://doi.org/10.1109/ISGTEurope.2013.6695235.
[8] Li R, Wang W, Xia M. Cooperative Planning of Active Distribution System with Renewable Energy Sources and Energy Storage Systems. IEEE Access 2017;6:5916–26. https://doi.org/10.1109/ACCESS.2017.2785263.
[9] Hooshmand E, Rabiee A. Robust model for optimal allocation of renewable energy sources, energy storage systems and demand response in distribution systems via information gap decision theory. IET Gener Transm Distrib 2019;13:511–20. https://doi.org/10.1049/iet-gtd.2018.5671.
[10] Disaster Data & Statistics. Natl Disaster Manag Auth n.d. https://ndma.gov.in/en/.
[11] Shen L, Cassottana B, Tang LC. Statistical trend tests for resilience of power systems. Reliab Eng Syst Saf 2018;177:138–47. https://doi.org/10.1016/j.ress.2018.05.006.
[12] Xue J, Mohammadi F, Li X, Sahraei-Ardakani M, Ou G, Pu Z. Impact of transmission tower-line interaction to the bulk power system during hurricane. Reliab Eng Syst Saf 2020;203. https://doi.org/10.1016/j.ress.2020.107079.
[13] NRSC/ISRO. Chennai Floods, 2015. [A Satellite and Field Based Assessment Study]; 2015.
[14] Mohamed MA, Chen T, Su W, Jin T. Proactive Resilience of Power Systems against Natural Disasters: A Literature Review. IEEE Access 2019;7:163778–95. https://doi.org/10.1109/ACCESS.2019.2952362.
[15] Lin Y, Bie Z, Qiu A. A review of key strategies in realizing power system resilience. Glob Energy Interconnect 2018;1:70–8. https://doi.org/10.14171/j.2096-5117.gei.2018.01.009.
[16] Birnie DP. Optimal battery sizing for storm-resilient photovoltaic power island systems. Sol Energy 2014;109:165–73. https://doi.org/10.1016/j.solener.2014.08.016.
[17] Nikkhah S, Jalilpoor K, Kianmehr E, Gharehpetian GB. Optimal wind turbine allocation and network reconfiguration for enhancing resiliency of system after major faults caused by natural disaster considering uncertainty. IET Renew Power Gener 2018;12:1413–23. https://doi.org/10.1049/iet-rpg.2018.5237.
[18] Yadav M, Pal N, Saini DK. Microgrid Control, Storage, and Communication Strategies to Enhance Resiliency for Survival of Critical Load. IEEE Access 2020;8:169047–69. https://doi.org/10.1109/access.2020.3023087.
[19] Najarian M, Lim GJ. Optimizing infrastructure resilience under budgetary constraint. Reliab Eng Syst Saf 2020;198. https://doi.org/10.1016/j.ress.2020.106801.
[20] Fang Y, Sansavini G. Optimizing power system investments and resilience against attacks. Reliab Eng Syst Saf 2017;159:161–73. https://doi.org/10.1016/j.ress.2016.10.028.
[21] Moradijoz M, Moradijoz S, Moghaddam MP, Haghifam MR. Flexibility enhancement in active distribution networks through a risk-based optimal placement of sectionalizing switches. Reliab Eng Syst Saf 2020;201. https://doi.org/10.1016/j.ress.2020.106985.
[22] Zhu H, Zhang C. Expanding a complex networked system for enhancing its reliability evaluated by a new efficient approach. Reliab Eng Syst Saf 2019;188:205–20. https://doi.org/10.1016/j.ress.2019.03.029.
[23] Toroghi SSH, Thomas VM. A framework for the resilience analysis of electric infrastructure systems including temporary generation systems. Reliab Eng Syst Saf 2020;202:107013. https://doi.org/10.1016/j.ress.2020.107013.
[24] Zhang B, Dehghanian P, Kezunovic M. Optimal Allocation of PV Generation and Battery Storage for Enhanced Resilience. IEEE Trans Smart Grid 2019;10:535–45. https://doi.org/10.1109/TSG.2017.2747136.
[25] Anuranj NJ, Mathew RK, Ashok S, Kumaravel S. Resiliency based power restoration in distribution systems using microgrids. In: 2016 IEEE 6th Int Conf Power Syst ICPS. 2016; 2016. p. 1–5. https://doi.org/10.1109/ICPES.2016.7584186.
[26] Balasubramaniam K, Saraf P, Hadidi R, Makram EB. Energy management system for enhanced resiliency of microgrids during islanded operation. Electr Power Syst Res 2016;137:133–41. https://doi.org/10.1016/j.epsr.2016.04.006.
[27] Yuan C, Illindala MS, Khalsa AS. Modified viterbi algorithm based distribution system restoration strategy for grid resiliency. IEEE Trans Power Deliv 2017;32:310–9. https://doi.org/10.1109/TPWRD.2016.2613935.
[28] Hussain A, Bui V, Kim H. Fuzzy Logic-Based Operation of Battery Energy Storage Systems (BESSs) for Enhancing the Resiliency of Hybrid Microgrids. Energies 2017;10:271. https://doi.org/10.3390/en10030271.
[29] Liu X, Shahidehpour M, Li Z, Liu X, Cao Y, Bie Z. Microgrids for Enhancing the Power Grid Resilience in Extreme Conditions. IEEE Trans Smart Grid 2017;8:589–97. https://doi.org/10.1109/TSG.2016.2579999.
[30] Hussain A, Bui VH, Kim HM. A proactive and survivability-constrained operation strategy for enhancing resilience of microgrids using energy storage system. IEEE Access 2018;6:75495–507. https://doi.org/10.1109/ACCESS.2018.2883418.
[31] Khederzadeh M, Zandi S. Enhancement of Distribution System Restoration Capability in Single/Multiple Faults by Using Microgrids as a Resiliency Resource. IEEE Syst J 2019;13:1796–803. https://doi.org/10.1109/JSYST.2019.2890898.
[32] Zhu J, Yuan Y, Wang W. An exact microgrid formation model for load restoration in resilient distribution system. Int J Electr Power Energy Syst 2020;116:105568. https://doi.org/10.1016/j.ijepes.2019.105568.
[33] Gilani MA, Kazemi A, Ghasemi M. Distribution system resilience enhancement by microgrid formation considering distributed energy resources. Energy 2020;191:116442. https://doi.org/10.1016/j.energy.2019.116442.
[34] Hughes W, Zhang W, Bagtzoglou AC, Wanik D, Pensado O, Yuan H, et al. Damage modeling framework for resilience hardening strategy for overhead power distribution systems. Reliab Eng Syst Saf 2021;207. https://doi.org/10.1016/j.ress.2020.107367.
[35] Salman AM, Li Y, Stewart MG. Evaluating system reliability and targeted hardening strategies of power distribution systems subjected to hurricanes. Reliab Eng Syst Saf 2015;144:319–33. https://doi.org/10.1016/j.ress.2015.07.028.
[36] Nazemi M, Moeini-Aghtaie M, Fotuhi-Firuzabad M, Dehghanian P. Energy Storage Planning for Enhanced Resilience of Power Distribution Networks Against Earthquakes. IEEE Trans Sustain Energy 2020;11:795–806. https://doi.org/10.1109/TSTE.2019.2907613.
[37] Sharma N, Tabandeh A, Gardoni P. Regional resilience analysis: A multiscale approach to optimize the resilience of interdependent infrastructure. Comput Civ Infrastruct Eng 2020;35:1315–30. https://doi.org/10.1111/mice.12606.
[38] Balaji Venkateswaran V, Saini DK, Sharma M. Approaches for optimal planning of the energy storage units in distribution network and their impacts on system resiliency. CSEE J Power Energy Syst 2020. https://doi.org/10.17775/CSEEJPES.2019.01280.
[39] Abdmouleh Z, Gastli A, Ben-Brahim L, Haouari M, Al-Emadi NA. Review of optimization techniques applied for the integration of distributed generation from renewable energy sources. Renew Energy 2017;113:266–80. https://doi.org/10.1016/j.renene.2017.05.087.
[40] Venkateswaran VB, Saini DK, Sharma M. Environmental Constrained Optimal Hybrid Energy Storage System Planning for an Indian Distribution Network. IEEE Access 2020;8:97793–808. https://doi.org/10.1109/ACCESS.2020.2997338.
[41] UPCL. Grid Map of Dehradun n.d. https://www.upcl.org/wss/downloads/dist_power_maps/dehradun.html.
[42] Joshi A, Kumar A, Castanos H, Lomnitz C. Seismic hazard of the Uttarakhand Himalaya, India, from deterministic modeling of possible rupture planes in the area. Int J Geophys 2013;2013. https://doi.org/10.1155/2013/825276.

[43] Multi-hazard loss estimation methodology: Earthquake model. 2003.
[44] Trakas DN, Hatziargyriou ND. Optimal Distribution System Operation for Enhancing Resilience Against Wildfires. IEEE Trans Power Syst 2018;33:2260–71. https://doi.org/10.1109/TPWRS.2017.2733224.
[45] BV V, Saini DK, Sharma M. Environmental Constrained Optimal Hybrid Energy Storage System Planning for an Indian Distribution Network. IEEE Access 2020. https://doi.org/10.1109/ACCESS.2020.2997338. 1–1.
[46] Irene H, Sandy S, Soudelor T, States U. Resilience-Oriented Pre-Hurricane Resource Allocation in Distribution Systems Considering Electric Buses 2017;105. https://doi.org/10.1109/JPROC.2017.2666548.
[47] Bhusal N, Abdelmalak M, Kamruzzaman M, Benidris M. Power system resilience: Current practices, challenges, and future directions. IEEE Access 2020;8:18064–86. https://doi.org/10.1109/ACCESS.2020.2968586.
[48] Panteli M, Pickering C, Wilkinson S, Dawson R, Mancarella P. Power System Resilience to Extreme Weather: Fragility Modeling, Probabilistic Impact Assessment, and Adaptation Measures. IEEE Trans Power Syst 2017;32:3747–57. https://doi.org/10.1109/TPWRS.2016.2641463.
[49] Federal Emergency Management Agency. Multi-hazard Loss Estimation Methodology - Earthquake Model. n.d.
[50] Li M, Hu JJ, Xie LL. Near-Fault Horizontal Peak Ground Acceleration and Velocity. In: 14 World Conf. Earthq. Eng; 2008.
[51] National Center for Seismology. Earthquakes in India. Minist Earth Sci Gov India n. d.
[52] Baumann M, Peters JF, Weil M, Grunwald A. CO 2 Footprint and Life-Cycle Costs of Electrochemical Energy Storage for Stationary Grid Applications. Energy Technol 2017;5:1071–83. https://doi.org/10.1002/ente.201600622.
[53] UPCL. In: Uttarakhand Electricity Regulatory Commission; 2019.